HOKKAIDO UNIVERSITY

Title	Multiple resonant coupling mechanism for suppression of higher-order modes in all-solid photonic bandgap fibers with heterostructured cladding
Author(s)	Murao, Tadashi; Saitoh, Kunimasa; Koshiba, Masanori
Citation	Optics Express, 19(3), 1713-1727 https://doi.org/10.1364/OE.19.001713
Issue Date	2011-01-31
Doc URL	https://hdl.handle.net/2115/45036
Rights	© 2011 Optical Society of America
Type	journal article
File Information	OE19-3_1713-1727.pdf

Hokkaido University Collection of Scholarly and Academic Papers : HUSCAP

Multiple resonant coupling mechanism for suppression of higher-order modes in all-solid photonic bandgap fibers with heterostructured cladding

Tadashi Murao,* Kunimasa Saitoh, and Masanori Koshiba

Graduate School of Information Science and Technology, Hokkaido University, Sapporo 060-0814, Japan
**murao@icp.ist.hokudai.ac.jp*

Abstract: In this paper, we propose a novel mechanism for suppression of higher-order modes (HOMs), namely multiple resonant coupling, in all-solid photonic bandgap fibers (PBGFs) with effectively large core diameters. In an analogy to the well-known tight-binding theory in solid-state physics, multiple anti-resonant reflecting optical waveguide (ARROW) modes bound in designedly arranged defects in the cladding make up Bloch states and resultant photonic bands with a finite effective-index width, which contribute to the suppression of HOMs. In particular, contrary to the conventional method for the HOM suppression using the index-matching of the HOMs in the core of the PBGF and the defect mode arranged in the cladding, the proposed mechanism guarantees a broadband HOM suppression without a precise structural design. This effect is explained by the multiple resonant coupling, as well as an enhanced confinement loss mechanism which occurs near the condition satisfying the multiple resonant coupling. Moreover, we show that the proposed structure exhibits a lower bending loss characteristic when compared to the conventional all-solid PBGFs. The simultaneous realization of the single-mode operation and the low bending loss property is due to the novel cladding concept named as heterostructured cladding. The proposed structure also resolves the issue for the increased confinement loss property in the first-order photonic bandgap (PBG) at the same time.

©2011 Optical Society of America

OCIS codes: (060.2280) Fiber design and fabrication; (060.2310) Fiber optics; (060.2400) Fiber properties; (060.5295) Photonic crystal fibers.

References and links

1. J. C. Knight, F. Luan, G. J. Pearce, A. Wang, T. A. Birks, and D. M. Bird, "Solid photonic bandgap fibres and applications," Jpn. J. Appl. Phys. **45**(No. 8A), 6059–6063 (2006).
2. F. Luan, A. K. George, T. D. Hedley, G. J. Pearce, D. M. Bird, J. C. Knight, and P. St. J. Russell, "All-solid photonic bandgap fiber," Opt. Lett. **29**(20), 2369–2371 (2004).
3. A. Argyros, T. A. Birks, S. G. Leon-Saval, C. M. B. Cordeiro, F. Luan, and P. St. J. Russell, "Photonic bandgap with an index step of one percent," Opt. Express **13**(1), 309–314 (2005).
4. A. Argyros, T. A. Birks, S. G. Leon-Saval, C. M. B. Cordeiro, and P. St J Russell, "Guidance properties of low-contrast photonic bandgap fibres," Opt. Express **13**(7), 2503–2511 (2005).
5. G. Bouwmans, L. Bigot, Y. Quiquempois, F. Lopez, L. Provino, and M. Douay, "Fabrication and characterization of an all-solid 2D photonic bandgap fiber with a low-loss region (< 20 dB/km) around 1550 nm," Opt. Express **13**(21), 8452–8459 (2005).
6. A. Wang, A. K. George, and J. C. Knight, "Three-level neodymium fiber laser incorporating photonic bandgap fiber," Opt. Lett. **31**(10), 1388–1390 (2006).
7. J. M. Stone, G. J. Pearce, F. Luan, T. A. Birks, J. C. Knight, A. K. George, and D. M. Bird, "An improved photonic bandgap fiber based on an array of rings," Opt. Express **14**(13), 6291–6296 (2006).
8. G. Ren, P. Shum, L. Zhang, X. Yu, W. Tong, and J. Luo, "Low-loss all-solid photonic bandgap fiber," Opt. Lett. **32**(9), 1023–1025 (2007).

#136546 - $15.00 USD Received 13 Oct 2010; revised 30 Dec 2010; accepted 11 Jan 2011; published 14 Jan 2011

9. R. Goto, K. Takenaga, S. Matsuo, and K. Himeno, "Solid photonic band-gap fiber with 400 nm bandwidth and loss below 4 dB/km at 1520 nm," in *Proceedings of 2007 Optical Fiber Communication Conference and Exposition/National Fiber Optic Engineers Conference (OFC/NFOEC)*, OML7 (2007).
10. T. Taru, J. Hou, and J. C. Knight, "Raman gain suppression in all-solid photonic bandgap fiber," in *Proceedings of 2007 European Conference on Optical Communication (ECOC)*, 7.1.1 (2007).
11. A. Bétourné, V. Pureur, G. Bouwmans, Y. Quiquempois, L. Bigot, M. Perrin, and M. Douay, "Solid photonic bandgap fiber assisted by an extra air-clad structure for low-loss operation around 1.5 μm," Opt. Express **15**(2), 316–324 (2007).
12. A. Bétourné, G. Bouwmans, Y. Quiquempois, M. Perrin, and M. Douay, "Improvements of solid-core photonic bandgap fibers by means of interstitial air holes," Opt. Lett. **32**(12), 1719–1721 (2007).
13. V. Pureur, L. Bigot, G. Bouwmans, Y. Quiquempois, M. Douay, and Y. Jaouen, "Ytterbium-doped solid core photonic bandgap fiber for laser operation around 980 nm," Appl. Phys. Lett. **92**(6), 061113 (2008).
14. C. B. Olausson, C. I. Falk, J. K. Lyngsø, B. B. Jensen, K. T. Therkildsen, J. W. Thomsen, K. P. Hansen, A. Bjarklev, and J. Broeng, "Amplification and ASE suppression in a polarization-maintaining ytterbium-doped all-solid photonic bandgap fibre," Opt. Express **16**(18), 13657–13662 (2008).
15. A. Shirakawa, H. Maruyama, K. Ueda, C. B. Olausson, J. K. Lyngsø, and J. Broeng, "High-power Yb-doped photonic bandgap fiber amplifier at 1150-1200 nm," Opt. Express **17**(2), 447–454 (2009).
16. V. Pureur, J. C. Knight, and B. T. Kuhlmey, "Higher order guided mode propagation in solid-core photonic bandgap fibers," Opt. Express **18**(9), 8906–8915 (2010).
17. N. M. Litchinitser, S. C. Dunn, P. E. Steinvurzel, B. J. Eggleton, T. P. White, R. C. McPhedran, and C. M. de Sterke, "Application of an ARROW model for designing tunable photonic devices," Opt. Express **12**(8), 1540–1550 (2004).
18. T. T. Larsen, A. Bjarklev, D. S. Hermann, and J. Broeng, "Optical devices based on liquid crystal photonic bandgap fibres," Opt. Express **11**(20), 2589–2596 (2003).
19. T. T. Alkeskjold, J. Lægsgaard, A. Bjarklev, D. S. Hermann, A. Anawati, J. Broeng, J. Li, and S. T. Wu, "All-optical modulation in dye-doped nematic liquid crystal photonic bandgap fibers," Opt. Express **12**(24), 5857–5871 (2004).
20. M. W. Haakestad, T. T. Alkeskjold, M. D. Nielsen, L. Scolari, J. Riishede, H. E. Engan, and A. Bjarklev, "Electrically tunable photonic bandgap guidance in a liquid-crystal-filled photonic crystal fiber," IEEE Photon. Technol. Lett. **17**(4), 819–821 (2005).
21. T. T. Alkeskjold, and A. Bjarklev, "Electrically controlled broadband liquid crystal photonic bandgap fiber polarimeter," Opt. Lett. **32**(12), 1707–1709 (2007).
22. J. Lægsgaard, "Gap formation and guided modes in photonic bandgap fibres with high-index rods," J. Opt. A: Pure Appl. Opt. **6**, 798–804 (2004).
23. M. A. Duguay, Y. Kokubun, T. L. Koch, and L. Pfeiffer, "Antiresonant reflecting optical waveguides in SiO_2-Si multilayer structures," Appl. Phys. Lett. **49**(1), 13–15 (1986).
24. T. Baba, Y. Kokubun, T. Sakaki, and K. Iga, "Loss reduction of an ARROW waveguide in shorter wavelength and its stack configuration," J. Lightwave Technol. **6**(9), 1440–1445 (1988).
25. N. M. Litchinitser, S. C. Dunn, B. Usner, B. J. Eggleton, T. P. White, R. C. McPhedran, and C. M. de Sterke, "Resonances in microstructured optical waveguides," Opt. Express **11**(10), 1243–1251 (2003).
26. K. J. Rowland, S. Afshar V, and T. M. Monro, "Bandgaps and antiresonances in integrated-ARROWs and Bragg fibers; a simple model," Opt. Express **16**(22), 17935–17951 (2008).
27. T. A. Birks, F. Luan, G. J. Pearce, A. Wang, J. C. Knight, and D. M. Bird, "Bend loss in all-solid bandgap fibres," Opt. Express **14**(12), 5688–5698 (2006).
28. T. Murao, K. Nagao, K. Saitoh, and M. Koshiba, "Understanding formation of photonic bandgap edge for maximum propagation angle in all-solid photonic bandgap fibers," J. Opt. Soc. Am. B (accepted for publication).
29. T. Murao, K. Saitoh, and M. Koshiba, "Detailed theoretical investigation of bending properties in solid-core photonic bandgap fibers," Opt. Express **17**(9), 7615–7629 (2009).
30. T. Murao, K. Saitoh, T. Taru, T. Nagashima, K. Maeda, T. Sasaki, and M. Koshiba, "Bend-insensitive and effectively single-moded all-solid photonic bandgap fibers with heterostructured cladding," in *Proceedings of European Conference on Optical Communication (ECOC)*, 2.1.4 (2009).
31. K. Saitoh, N. J. Florous, T. Murao, and M. Koshiba, "Design of photonic band gap fibers with suppressed higher-order modes: towards the development of effectively single mode large hollow-core fiber platforms," Opt. Express **14**(16), 7342–7352 (2006).
32. J. M. Fini, "Aircore microstructure fibers with suppressed higher-order modes," Opt. Express **14**(23), 11354–11361 (2006).
33. K. Saitoh, and M. Koshiba, "Full-vectorial imaginary-distance beam propagation method based on a finite element scheme: Application to photonic crystal fibers," IEEE J. Quantum Electron. **38**(7), 927–933 (2002).
34. N. W. Ashcroft, and N. D. Mermin, *Solid state physics*, (Holt, Rinehart, and Winston, 1976).
35. J. D. Love, "Application of a low-loss criterion to optical waveguides and devices," IEE Proc. Pt. J **136**, 225–228 (1989).
36. T. A. Birks, G. J. Pearce, and D. M. Bird, "Approximate band structure calculation for photonic bandgap fibres," Opt. Express **14**(20), 9483–9490 (2006).
37. Z. Wang, T. Taru, T. A. Birks, J. C. Knight, Y. Liu, and J. Du, "Coupling in dual-core photonic bandgap fibers: theory and experiment," Opt. Express **15**(8), 4795–4803 (2007).
38. M. J. F. Digonnet, H. K. Kim, G. S. Kino, and S. Fan, "Understanding air-core photonic-bandgap fibers: Analogy to conventional fibers," J. Lightwave Technol. **23**(12), 4169–4177 (2005).

#136546 - $15.00 USD Received 13 Oct 2010; revised 30 Dec 2010; accepted 11 Jan 2011; published 14 Jan 2011
(C) 2011 OSA

39. Y. Li, C. Wang, T. A. Birks, and D. M. Bird, "Effective index method for all-solid photonic bandgap fibres," J. Opt. A: Pure Appl. Opt. **9**, 858–861 (2007).
40. T. Murao, K. Saitoh, K. Nagao, and M. Koshiba, "Design principle for low bending losses in all-solid photonic bandgap fibers," in *Proceedings of Conference on Lasers and Electro-Optics and Quantum Electronics and Laser Science Conference (CLEO/QELS 2010)*, paper JTuD45.

1. Introduction

Recently, all-solid photonic bandgap fibers (PBGFs) [1–16], which are one of the types of solid-core PBGFs, have attracted considerable attention due to their unusual transmission characteristics which cannot be obtained by conventional optical fibers. In all-solid PBGFs, the cladding is composed of periodically arranged high-index Ge-doped rods and the core is usually formed by omitting one rod. Owing to the photonic bandgap (PBG) effect of the photonic crystal structure for light with out-of-plane propagation, a fundamental core mode is supported in the defected core region with effectively low losses. Because of the functionality pattern of having alternate transmission and transmission-inhibited bands which the photonic-crystal cladding exhibits, the PBGFs can be applied to several devices. In particular, when compared to the other type of solid-core PBGFs whose high-index rods are composed of high-index liquid [17–21], because of its higher degree of compatibility with all-glass conventional fibers, the all-solid type can be easily incorporated into fiber amplifiers or fiber lasers as fiber-type optical filters, taking advantage of the intriguing transmission band property.

The photonic crystal structure in the cladding of all-solid PBGFs generates a number of PBG orders separated by photonic bands associated with linearly polarized (LP) rod modes [22], according to the point of view of the anti-resonant reflecting optical waveguide (ARROW) theory [23–26]. It is known that, in general, odd-ordered PBGs have a deeper PBG depth when compared to even-ordered PBGs, partly because of their smaller modal overlap characteristic for rod modes concerning the blue edge, which results in the less effect of the enlargement of the band width on the PBG edge [22,27]. In addition to this, because the LP modes bound in high-index rods are symmetrical at the edge of the even-ordered PBGs, a factor responsible for increasing the PBG depth becomes small, which has a relation with a transverse wave vector component of the Bloch state corresponding to the PBG edge. On the other hand, because the component becomes larger for the case in the odd-ordered PBGs where the LP rod modes are anti-symmetrical, the odd-ordered PBGs have a deeper PBG depth [28]. Among all of the odd-ordered PBGs, the third-order PBG supports a lower confinement loss property than the first-order PBG [5] because the propagation angle for the core modes is lower in the third-order PBG; in other words, the core radius relative to wavelength is larger in most cases. However, because the single-mode operation for the structure utilizing the third-order PBG with the larger core radius relative to wavelength is due to the shallower PBG depth as compared to the first-order PBG, exploitation of the third-order PBG causes a high bending loss in general. Accordingly, there have been several attempts to resolve the issue; by removing the modes bound in high-index rods which degrade the bending loss property based on an array of rings [7], by incorporating air holes surrounding the photonic-crystal structure [11], and by decreasing the width of photonic bands and, therefore, increasing the PBG depth with arranged interstitial air holes surrounding each high-index rod [12].

On the other hand, the exploitation of the first-order PBG has also been considered employing the structure with a reduced confinement loss by simply approaching the condition of the multi-mode operation [8,9]. In fact, recently we have shown that the first-order PBG exhibits a lower bending loss property than the third-order PBG even if the core radius relative to wavelength is smaller (therefore the effective index of the core mode is smaller) due to its deeper PBG depth [29]. Moreover, adopting the 7-cell-core structure in the first-order PBG, which has almost the same core radius as the 1-cell-core structure exploiting the third-order PBG, is more beneficial for reducing the bending loss, as well as the confinement loss. This fact leads to resolving the issue for utilizing the first-order PBG. However, the 7-cell-core PBGF in the first-order PBG operates in a multi mode due to the deep PBG depth. In order to take advantage of this structure, there is a necessary requirement that the 7-cell-core

#136546 - $15.00 USD Received 13 Oct 2010; revised 30 Dec 2010; accepted 11 Jan 2011; published 14 Jan 2011
(C) 2011 OSA

PBGF operates in a single mode at the first-order PBG without degradation of the bending property such as a critical bend radius [29,30].

In order to suppress higher-order modes (HOMs) from an effectively large core, a method has been proposed which takes advantage of the index-matching between the HOMs of the PBGF and the defect mode arranged in the cladding [31,32]. In general, an asymmetric directional-coupler structure, however, leads to a narrow operational bandwidth. Although the dispersion relations between the HOM of the PBGF and the defect mode exhibit an analogous tendency in wavelength to some extent [32], in order to satisfy the index-matching to realize the HOM suppression properly and to prevent the narrowband operation, an effort for the precise structural design is required. This fact has been one of the issues for such a structure.

In this paper, we propose a novel mechanism for suppression of HOMs, namely multiple resonant coupling, in all-solid PBGFs with effectively large core diameters, which enables a single mode operation at the first-order PBG without degradation of the bending property. In an analogy to the well-known tight-binding theory in solid-state physics, multiple ARROW modes bound in designedly arranged defects as a triangular lattice in the cladding make up Bloch states and resultant photonic bands with a finite effective-index width, which contribute to the suppression of HOMs. In particular, contrary to the conventional method for the HOM suppression using the index-matching of the HOMs in the core of the PBGF and the defect mode arranged in the cladding, the proposed mechanism guarantees a broadband HOM suppression without a precise design of the defected cores set in the cladding. This effect is explained by the multiple resonant coupling, as well as an enhanced confinement loss mechanism which occurs near the condition satisfying the multiple resonant coupling. Moreover, we show that the proposed structure exhibits a lower bending loss characteristic when compared to the conventional all-solid PBGFs. The simultaneous realization of the single-mode operation and the low bending loss property is due to the novel cladding concept named as heterostructured cladding [30], which is also reviewed in detail in this paper. The proposed structure also resolves the issue for the increased confinement loss property in the first-order PBG at the same time, without any particular complicated fabrication techniques except for the stack-and-draw ones.

The contents in this paper are arranged as follows. In Sec. 2, we present a fundamental concept of the multiple resonant coupling for the HOM suppression. Next, by considering two divided cladding sections of the proposed structure (namely heterostructured cladding), the novel mechanism is explained in detail, as well as important roles of the heterostructured cladding in Sec. 3.

2. Concept of multiple resonant coupling mechanism

The cladding of typical all-solid PBGFs is composed of a periodic arrangement of high-index rods in a low-index silica background structured as a triangular lattice. Figure 1 shows cross sections of the typical all-solid PBGF (named as “uniform” structure) with 1-cell core and 7 cladding rings in (a), and 7-cell core and 6 cladding rings (keeping the cladding region when compared to the fiber with 1-cell core and 7 cladding rings) in (b). In this figure, *d* stands for

#136546 - $15.00 USD Received 13 Oct 2010; revised 30 Dec 2010; accepted 11 Jan 2011; published 14 Jan 2011
(C) 2011 OSA

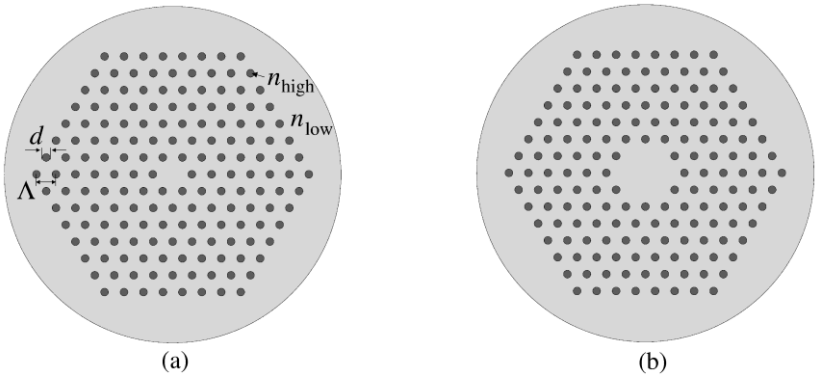

Fig. 1. Cross sections of typical all-solid PBGF ("uniform" structure) with (a) 1-cell core and 7 rings, and (b) 7-cell core with 6 rings (cladding region is in keeping with that of the fiber with 1-cell core and 7 rings), where d stands for diameter of high-index rods, Λ is the distance between adjacent rods, and n_{high}, n_{low} are refractive indices of high-index rods and low-index background, respectively. Unless the exceptional clause is shown, the structural parameters of $d/\Lambda = 0.4$, $\Lambda = 7.0$ μm, $n_{high} = 1.48$, and $n_{low} = 1.45$ are considered.

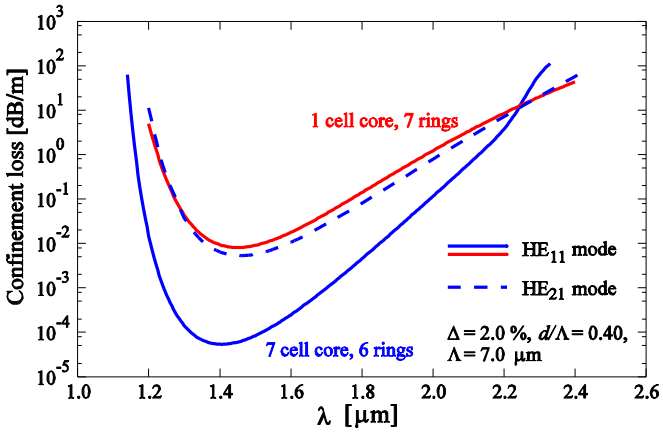

Fig. 2. Confinement losses as a function of wavelength for uniform 1-cell-core structure (red curve) and 7-cell-core structure (blue curves) in the first-order PBG. Exploiting the 7-cell-core structure in the first-order PBG also leads to the improvement of the confinement loss property as well as the bending loss property, while causing the multi-mode operation.

the diameter of the high-index rods, Λ is the distance between adjacent rods, and n_{high}, n_{low} are the refractive indices of the high-index rods and the low-index background, respectively. Unless otherwise specified, we choose the structural parameters as $d/\Lambda = 0.4$, $\Lambda = 7.0$ μm, $n_{high} = 1.48$, and $n_{low} = 1.45$ (the relative refractive index difference $\Delta = 2\%$) as commonly-used parameters to set the mid-gap wavelength of the first-order PBG in 1.55 μm and let a low confinement loss property be compatible with a low bending loss property to some extent for the 1-cell-core structure. Recently, we have shown that the structure utilizing the first-order PBG exhibits an apparently lower bending loss property than that using the third-order PBG for the typical 1-cell-core structure. However, it does at the expense of the higher confinement loss property due to the larger propagation angle caused by the smaller core radius relative to wavelength in the first-order PBG [29]. Moreover, the enlargement of the core radius as in the 7-cell-core structure has a remarkable benefit for reducing the bending loss in the first-order PBG [29]. In Fig. 2, the confinement losses as a function of wavelength in the first-order PBG are presented for the 1-cell-core structure (red curve) and the 7-cell-core structure (blue curves), calculated by using the vector finite element method (FEM) [33]. It is noted that the

#136546 - $15.00 USD Received 13 Oct 2010; revised 30 Dec 2010; accepted 11 Jan 2011; published 14 Jan 2011
(C) 2011 OSA

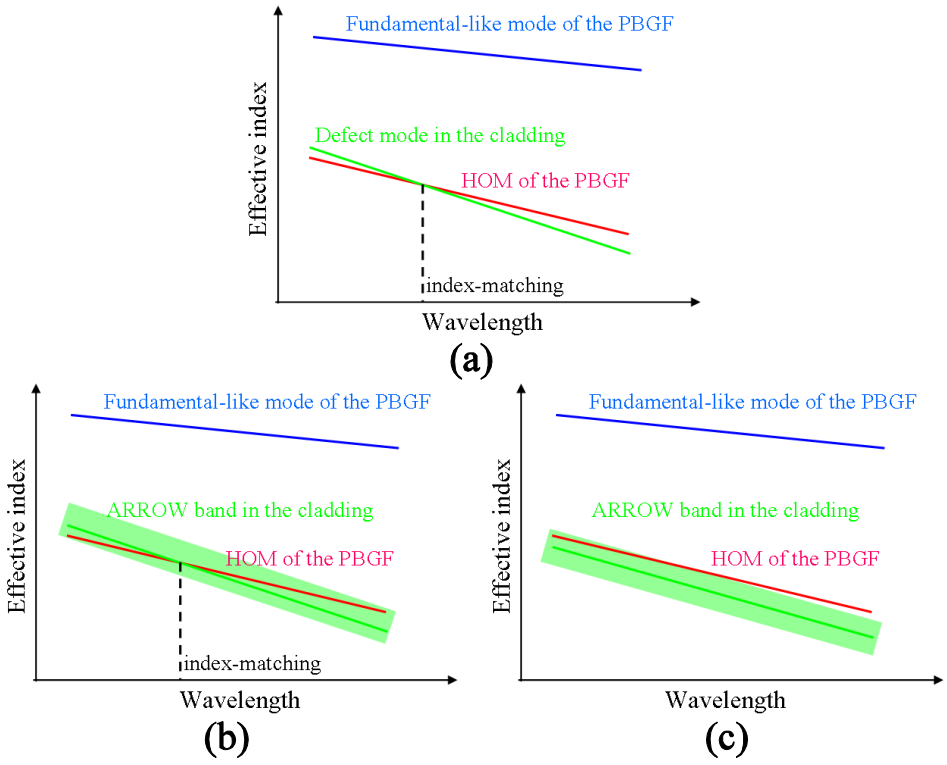

Fig. 3. Schematic representation of the dispersion relation for (a) the conventional HOM suppression method based on index-matching operating at only a particular wavelength that index-matching occurs, (b) the proposed method based on multiple resonant coupling operating for a wide wavelength range owing to photonic bands generated by ARROW modes in the cladding, and (c) the enhanced confinement loss mechanism which supports the HOM suppression at the condition that multiple resonant coupling does not occur.

enlargement of the core radius also leads to the improvement of the confinement loss property and, therefore, resolving the issue for exploiting the first-order PBG, as well as reducing the bending loss, due to the increment of the effective index. In this case, however, although the core radius relative to wavelength is almost the same as the 1-cell-core structure utilizing the third-order PBG, the HOMs are also supported because of its deeper PBG depth than the third-order one (in Fig. 2, only the HE_{21} mode is depicted as the second-order mode, because the other modes exhibit the same tendency). Here, we propose a novel structure which suppresses the HOMs while at the same time suites the requirement for the low bending loss property.

The schematic representation of the dispersion relation for the conventional HOM suppression method based on index-matching [31,32] is depicted in Fig. 3(a). In this method, a few additional cores which are incorporated into the fiber cladding induce a high confinement loss for HOMs of the PBGF at only a particular wavelength that index-matching occurs. Although it is known that the dispersion relations between the HOM of the PBGF and the defect mode exhibit an analogous tendency in wavelength to some extent [32], in order to satisfy the index-matching to realize the HOM suppression properly and to prevent the narrowband operation, an effort for the precise structural design is required. In order to resolve the issue, we propose a novel structure shown in Fig. 4(a), where the multiple cores are formed by omitting the high-index rods from the uniform triangular lattice structure. We note that the multiple outer cores in the cladding are also periodically aligned to be the triangular lattice structure. The schematic representation of the dispersion relation for the proposed structure is depicted in Fig. 3(b). The fundamental-like core mode is supported due

#136546 - $15.00 USD Received 13 Oct 2010; revised 30 Dec 2010; accepted 11 Jan 2011; published 14 Jan 2011
(C) 2011 OSA

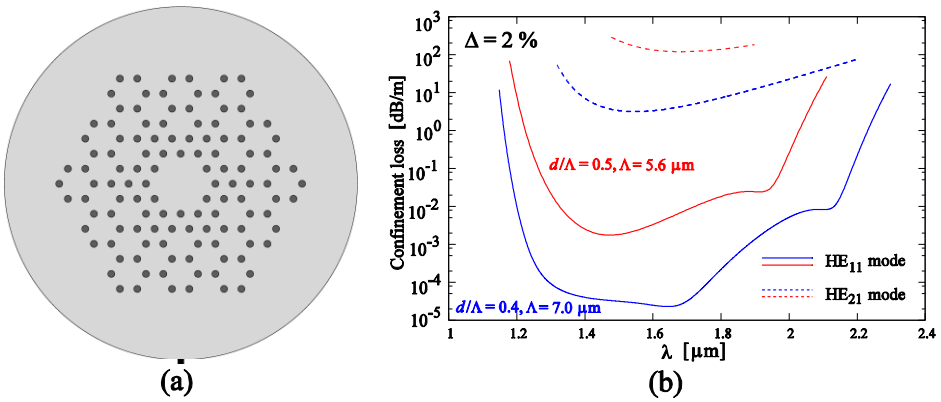

Fig. 4. (a) Cross section for the proposed all-solid PBGF which satisfies the multiple resonant coupling shown in Fig. 3(b) or enhanced confinement loss mechanism shown in Fig. 3(c). The cladding has periodically arranged multiple cores. (b) Confinement losses as a function of wavelength for the proposed structure with 6 cladding rings. The HOM is effectively suppressed while keeping the confinement loss low for the fundamental-like mode for d/Λ = 0.4 and Λ = 7.0 μm (blue curves), as well as for d/Λ = 0.5 and Λ = 5.6 μm (red curves).

to the ARROW condition for each high-index rod in the cladding. Moreover, it is worth noting that periodically aligned modes bound in low-index regions in the cladding are also produced due to the ARROW condition for each six high-index rods surrounding a low-index region. That is, contrary to the conventional index-matching method, the modes bound in the periodic multiple outer cores form Bloch states and resultant photonic bands. In this case, because the operating suppression band is not limited to the condition that index-matching occurs due to the formed photonic band with a finite width, a wideband operation is expected. This phenomenon can also be intuitively understood by considering the analogy to the well-known tight-binding theory in solid-state physics [34]. If each isolated atom comes close each other, the large overlap of the wave functions causes an increment of the width of energy bands, where the overlap also produces a quantum tunneling effect. In the proposed structure, on the other hand, the HOMs satisfying the condition on photonic bands formed by the multiple outer cores are also immediately suppressed due to the resonant tunneling effect. It is also noted that even if an arbitrary fiber design does not satisfy the index-matching condition for all over the wavelength range as in Fig. 3(c), owing to the finite size of the cladding, an enhanced confinement loss mechanism occurs near photonic bands. Due to this effect, any effort for the precise structural design is not required contrary to the conventional index-matching method. In Fig. 4(b), we present confinement losses as a function of wavelength for the proposed structure shown in Fig. 4(a) with 6 cladding rings. We can see that the HOM is effectively suppressed for a wide wavelength range while keeping the confinement loss for the fundamental-like mode low as in the 7-cell-core structure shown in Fig. 2. Moreover, we confirmed that the condition of the HOM suppression for the proposed structure is apparently not sensitive to the structural parameters. As an example, the confinement losses for the fundamental-like mode and the HE_{21} mode at the mid-gap wavelength are about 2.1×10^{-3} dB/m and 158 dB/m, respectively, for d/Λ = 0.5, Λ = 5.6 μm, and Δ = 2% (d and Δ are the same as those considered above and only Λ is decreased) as shown in Fig. 4(b).

Moreover, because the 7-cell-core structure is adopted for the proposed fiber, it exhibits a lower bending loss property than the conventional all-solid PBGFs. In Fig. 5, the bending-radius dependence of the bending losses at λ = 1.55 μm is presented for the proposed structure shown in Fig. 4(a). Although the bending loss has a dependence of the bent direction in a precise sense, because it is not expected to make a significant difference on the result due to the rotational symmetry, it is set to the lateral direction of the cross section shown above. As a reference, results are also shown for the conventional 1-cell-core structure with triangular lattice cladding utilizing the first-order PBG shown in Fig. 1(a) and conventional 1-cell-core

#136546 - $15.00 USD Received 13 Oct 2010; revised 30 Dec 2010; accepted 11 Jan 2011; published 14 Jan 2011
(C) 2011 OSA

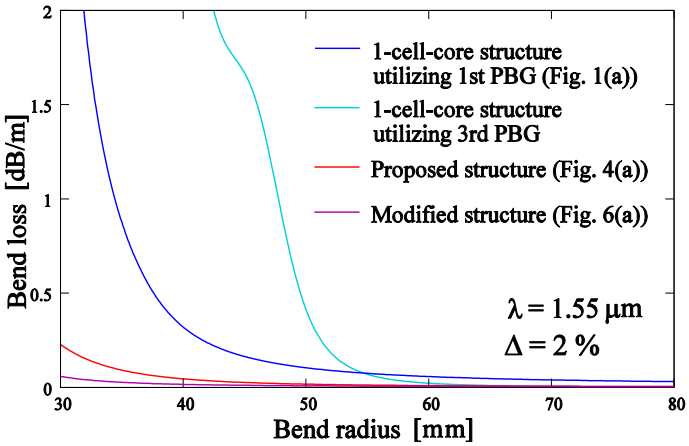

Fig. 5. Bending losses as function of bending radius at $\lambda = 1.55$ μm for the proposed structure shown in Fig. 4(a) (red curve) and modified structure shown in Fig. 6(a) (purple curve), where $d/\Lambda = 0.5$ and $\Lambda = 5.6$ μm. As a reference, results are also shown for conventional 1-cell-core structure with triangular lattice cladding utilizing the first-order PBG shown in Fig. 1(a) (blue curve), where $d/\Lambda = 0.4$ and $\Lambda = 7.0$ μm, and conventional 1-cell-core structure utilizing the third-order PBG (cyan curve). For the structure utilizing the third-order PBG, the parameters are chosen as $d/\Lambda = 0.56$ and $\Lambda = 13.5$ μm with 6 cladding rings.

structure utilizing the third-order PBG. Because the 1-cell-core structure utilizing the first-order PBG exhibits a high confinement loss property, the parameters are set to $d/\Lambda = 0.4$, $\Delta = 2\%$, and $\Lambda = 7.0$ μm as mentioned above. Concerning the proposed 7-cell-core structure with the heterostructured cladding, on the other hand, because of its lower confinement loss property, it is possible to decrease the pitch as $d/\Lambda = 0.5$, $\Delta = 2\%$, and $\Lambda = 5.6$ μm to obtain a low bending loss property, at the expense of the slight increment of the confinement loss for the fundamental-like mode (see Fig. 4(b)). For the 1-cell-core structure utilizing the third-order PBG, the structural parameters are chosen as $d/\Lambda = 0.56$, $\Delta = 2\%$, and $\Lambda = 13.5$ μm in order to set the mid-gap wavelength in 1.55 μm and to have a comparable core size relative to wavelength to the proposed structure (7-cell-core structure utilizing the first-order PBG). It is seen that the conventional 1-cell-core structure utilizing the third-order PBG clearly exhibits the highest bending loss property where the value increases at bending radius $R = 60$ mm. Although it seems that the 1-cell-core structure utilizing the first-order PBG exhibits a lower bending loss property, it also has the high confinement loss characteristic as explained above (see Fig. 2). In addition, the value of bending loss becomes more than 0.1 dB/m even at $R = 50$ mm as seen in Fig. 5. On the other hand, the structure utilizing the heterostructured cladding shown in Fig. 4(a) apparently exhibits the better bending loss characteristic.

It is also possible to design a fiber which exhibits a lower bending loss than the proposed structure shown in Fig. 4(a) furthermore. Actually, the aim of the proposed structure in this paper was to achieve a single-mode operation while avoiding the degradation of the great bending loss property in the first-order PBG of the multi-moded 7-cell-core uniform structure. However, the proposed structure exhibits a slightly higher bending loss. This is because of the fact that the larger gap between rods, as compared to the triangular lattice, causes resonances in the cladding when the fiber is bent. Surely, if high-index rods are embedded in the low-index regions of the cladding, it leads to a multi-mode operation for the 7-cell-core structure because the lattice structure comes close to the triangular lattice, while decreasing a bending loss. However, if the place in which high-index rods are embedded is appropriately chosen as the multiple resonant coupling occurs, it is possible to reduce the bending loss while less affecting the confinement loss of the HOMs. In Fig. 6(a) and (b), we present the cross section of the modified structure and the confinement losses of the guided modes, where the several low-index regions in the cladding are replaced with the high-index rods. In addition to this,

#136546 - $15.00 USD Received 13 Oct 2010; revised 30 Dec 2010; accepted 11 Jan 2011; published 14 Jan 2011
(C) 2011 OSA

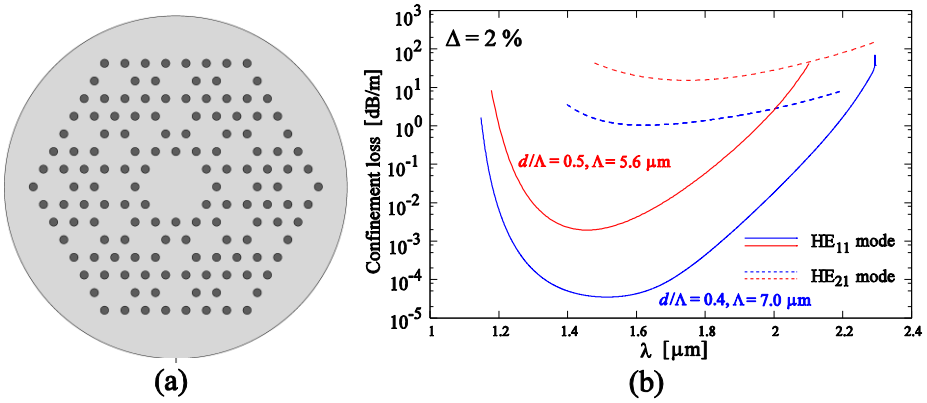

Fig. 6. (a) Cross section of the modified heterostructured PBGF, where the several high-index rods are embedded in the low-index regions designed as causing the multiple resonant coupling mechanism. (b) Confinement losses as a function of wavelength for the guided modes with 6 cladding rings. The HOM is effectively suppressed while keeping the confinement loss low for the fundamental-like mode for $d/\Lambda = 0.4$ and $\Lambda = 7.0$ μm (blue curves), as well as for $d/\Lambda = 0.5$ and $\Lambda = 5.6$ μm (red curves).

the number of the 1st cladding layers is also reduced to one to suppress the HOM sufficiently. It is noted that because the low-index regions are aligned with the one-dimensional arrangement in a radial fashion, the effect of the embedded high-index rods on the confinement of HOMs is small. In fact, the confinement loss for the HOM is more than 25 dB/m even at the mid-gap wavelength as shown in Fig. 6(b) for $d/\Lambda = 0.5$, $\Delta = 2\%$, and $\Lambda = 5.6$ μm. In Fig. 5, the bending-radius dependence of the bending losses at $\lambda = 1.55$ μm is also shown for the modified structure shown in Fig. 6(a). We can see that it clearly exhibits a very low bending loss property, while keeping the effectively single-mode operation. It is worth noting that the low bending loss properties for all the structures proposed here are simply realized by replacing several high-index rods into silica, contrary to the conventional structure which attempts to reduce the bending loss [8].

In general, it is important to see the effective index difference between the fundamental-like mode and the HOMs to avoid unwanted mode coupling due to undesired longitudinal variations caused by macro- and micro-bends, etc [35]. A small effective-index difference between them would also produce a large bending loss due to such a coupling. In the 7-cell-core structure utilizing the first-order PBG, however, because the core radius relative to wavelength is almost the same as the 1-cell-core structure utilizing the third-order PBG, the degree of the mode coupling in the proposed structures is considered to be almost the same as that in conventional single-mode all-solid PBGFs utilizing the third-order PBG (in this case, between the fundamental-like mode and the cladding modes).

Concerning the proposed mechanism shown above, having another point of view gives us an efficiently intuitive and detailed understanding, where the structure shown in Fig. 4(a) can be considered as a heterostructured cladding [30]. In the next section, we show the fundamental for the formation of the photonic bands generated by ARROW modes in the cladding and the concept of the novel cladding. In particular, we demonstrate that the heterostructured cladding is responsible for the simultaneous realization of the single-mode operation and the low bending loss property.

3. Understanding the proposed mechanism in more detail

3.1. Photonic band diagram for honeycomb structure

From the point of view of the novel cladding concept, the proposed structure shown in Fig. 4(a) is regarded as a heterostructured cladding composed of the honeycomb lattice for the 2nd cladding. By considering this, the photonic bands formed by ARROW modes in the cladding

#136546 - $15.00 USD Received 13 Oct 2010; revised 30 Dec 2010; accepted 11 Jan 2011; published 14 Jan 2011
(C) 2011 OSA

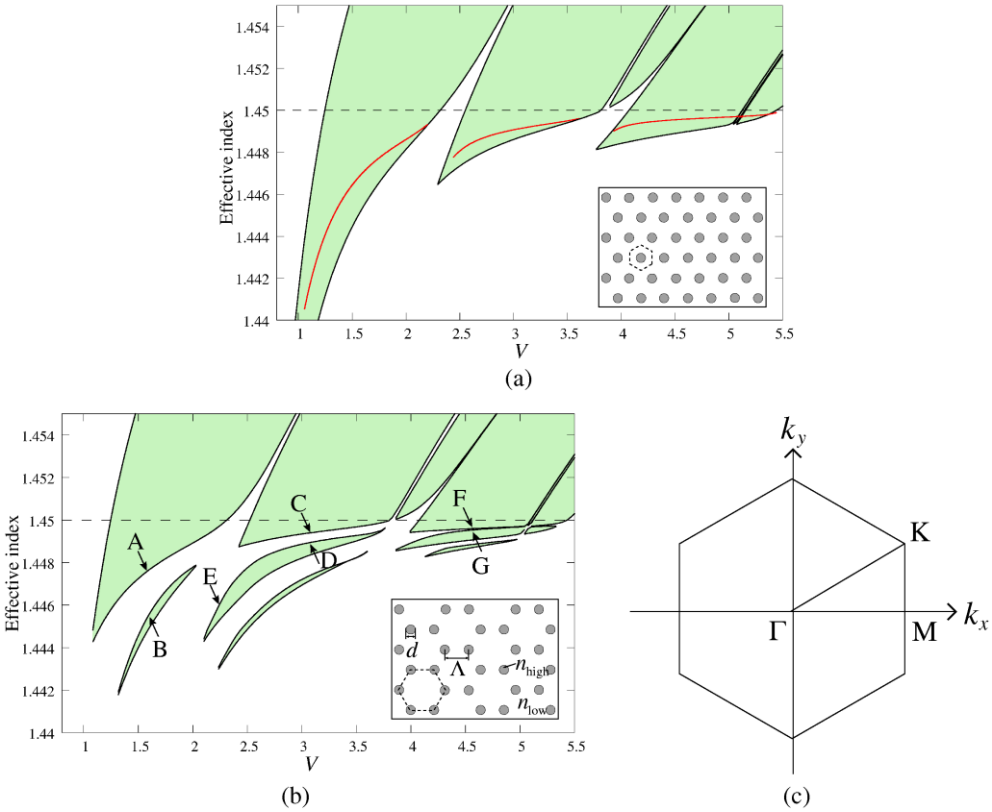

Fig. 7. Photonic band diagrams (green region) for the (a) triangular lattice and (b) honeycomb lattice for first, second, and third-order PBGs (from left to right), where red curves in (a) are dispersion curves of the fundamental-like mode for the 1-cell-core all-solid PBGF shown in Fig. 1(a) and the arrows in (b) correspond to the condition at which Bloch states will be presented in Fig. 8. The insets in (a) and (b) depict the corresponding lattice structure, where the hexagonal region stands for the unit cell. (c) First Brillouin zone boundary in reciprocal lattice space for two-dimensional triangular lattice with the pitch Λ', where (k_x, k_y) = (0, 0) at Γ point, (k_x, k_y) = $\left(2\pi/\sqrt{3}\Lambda', 0\right)$ at M point, and (k_x, k_y) = $\left(2\pi/\sqrt{3}\Lambda', 2\pi/3\Lambda'\right)$ at K point, where $\Lambda' = \sqrt{3}\Lambda$.

can efficiently be understood. According to the ARROW theory, because the transmission-inhibited bands of all-solid PBGFs are largely determined only by the values of d and Δ while not depending on the lattice constant [25], very few works address a utilization of another lattice structure except for the triangular lattice. However, according to the model which we established recently, the effective index of the PBG edge (or PBG depth) is determined by simply considering the transverse wave vector component corresponding to each Bloch state because a photonic-crystal cladding can be regarded as a homogeneous background material when the value of d/Λ is small ($d/\Lambda < 0.3$). Therefore, the PBG edge at a wavelength does not depend on the values of d and Δ and it is largely determined only by the lattice constant. Moreover, when the value of d/Λ is effectively large, the penetration of the modes bound in low-index regions into high-index rods is the major factor for increasing the effective index of the PBG edge [28]. This implies that it is also highly important to investigate photonic band diagrams for another lattice structure of high-index rods, as well as the conventional triangular lattice, from a scientific and technological point of view.

Figure 7(a) and (b) shows the photonic band diagrams for the triangular lattice and the honeycomb lattice, respectively, where V is the normalized frequency defined as follows;

#136546 - $15.00 USD Received 13 Oct 2010; revised 30 Dec 2010; accepted 11 Jan 2011; published 14 Jan 2011
(C) 2011 OSA

$$V = \frac{\pi d}{\lambda}\left(n_{high}^2 - n_{low}^2\right)^{1/2}. \quad (1)$$

here, because the honeycomb lattice is not Bravais lattice, the reciprocal lattice is defined with the aid of that of the triangular lattice with the pitch $\Lambda' = \sqrt{3}\Lambda$ as shown in Fig. 7(c), where $(k_x, k_y) = (0, 0)$ at Γ point, $(k_x, k_y) = \left(2\pi/\sqrt{3}\Lambda', 0\right)$ at M point, and $(k_x, k_y) = \left(2\pi/\sqrt{3}\Lambda', 2\pi/3\Lambda'\right)$ at K point. The red curves in Fig. 7(a) represents the dispersion curves for the fundamental-like core mode of the 1-cell-core all-solid PBGF shown in Fig. 1(a). The PBGs are separated for wavelengths determined by LP modes bound in high-index rods for the honeycomb structure, as well as for the triangular lattice as deduced by the ARROW theory [22]. This is because the high-index rods between them are absolutely the same except for the arrangement. Interestingly, another factor for the PBG separations emerges for the honeycomb lattice due to the difference in the condition of low-index regions. In fact, for the honeycomb lattice, it is observed that several photonic bands exist whose effective index for the highest one in each PBG is very close to that of the red curves shown in Fig. 7(a). In order to see this, one of the transverse electric field components (E_x) of Bloch states corresponding to the edge of the photonic bands (indicated by arrows from A to G in Fig. 7(b)) are presented in Fig. 8. It can be seen that the photonic bands are related to each ARROW mode supported in each low-index region surrounded by 6 high-index rods. According to Bloch theorem, a phase shift of a resonant mode from another is related to $\boldsymbol{k}\cdot\boldsymbol{R}$, where $\boldsymbol{k}$ stands for the wave vector in the first Brillouin zone and $\boldsymbol{R}$ for the translation vector [34]. For example in the first-order PBG, because the state indicated by A in Fig. 7(b) is related to K point, the phase shift for neighbor ARROW modes is $4\pi/3$ in Fig. 8(a) and, on the other hand, because the state indicated by B is related to Γ point, the phase shift for neighbor ARROW modes is 0.

It is noted that in the second and third-order PBGs, the photonic bands formed by higher-order ARROW modes also emerge. In an analogy to the tight-binding theory in solid-state physics where the energy band width becomes larger for the state corresponding to the higher atomic energy level [34], the photonic band width also increases for the state corresponding to the higher-order ARROW mode because of the lower localization characteristic in low-index regions. In conventional waveguide couplers with multiple cores, it is known that the effective index for the even state is higher than that for the odd state in general. We also note that if the state shown in Fig. 8 is considered as the mode for the ARROW-type coupler with 1-cell cores, the effective index for the odd state is higher than that for the even one in the odd-ordered PBGs, contrary to the case for conventional waveguides. In the triangular lattice case, it is known that the states corresponding to the PBG floor are determined by the rod modes hybridized with resonant states between rods [36]. In the honeycomb lattice case, the phenomenon is also explained by the analogy. Actually, this is due to the symmetrical reason of the LP mode bound in high-index rods as in the case for the triangular lattice [28]. Because the LP_{11} rod mode is the anti-symmetrical mode in rods, the resultant state for the low-index regions, which is responsible for the state A in Fig. 7(b) at the PBG edge, becomes odd when the anti-symmetrical mode in rods forms the even state. On the other hand, the photonic band edge indicated by B in Fig. 7(b) is formed by even state of LP_{02} rod modes, which are symmetrical in rods. This is due to the fact that, because the transverse wave vector component for the even state of the LP_{02} rod modes is small, it penetrates into the first-order PBG (as can also be seen by the diagram in Fig. 7(b) or by the rod modes' profile in Fig. 8(b)). Therefore, the resultant state for the low-index regions becomes even when the symmetrical mode in rods forms the even state, and so on. In particular, interestingly, the relation of even and odd states is conserved when the number of cores of ARROW is even decreased to 2 cores, as in the case for the bands formed by high-index rods [36]. In Fig. 9(a) and (b), we show the cross section of the conventional all-solid PBGF coupler with 2 cores and the dispersion curves for the even and odd modes, respectively. Apparently, we can see that the effective index for the odd mode is larger in the odd-ordered PBGs. This explains one

#136546 - $15.00 USD Received 13 Oct 2010; revised 30 Dec 2010; accepted 11 Jan 2011; published 14 Jan 2011
(C) 2011 OSA

of the critical reasons why the effective index for the odd mode can be larger in PBGFs, which has not been mentioned in Ref [37].

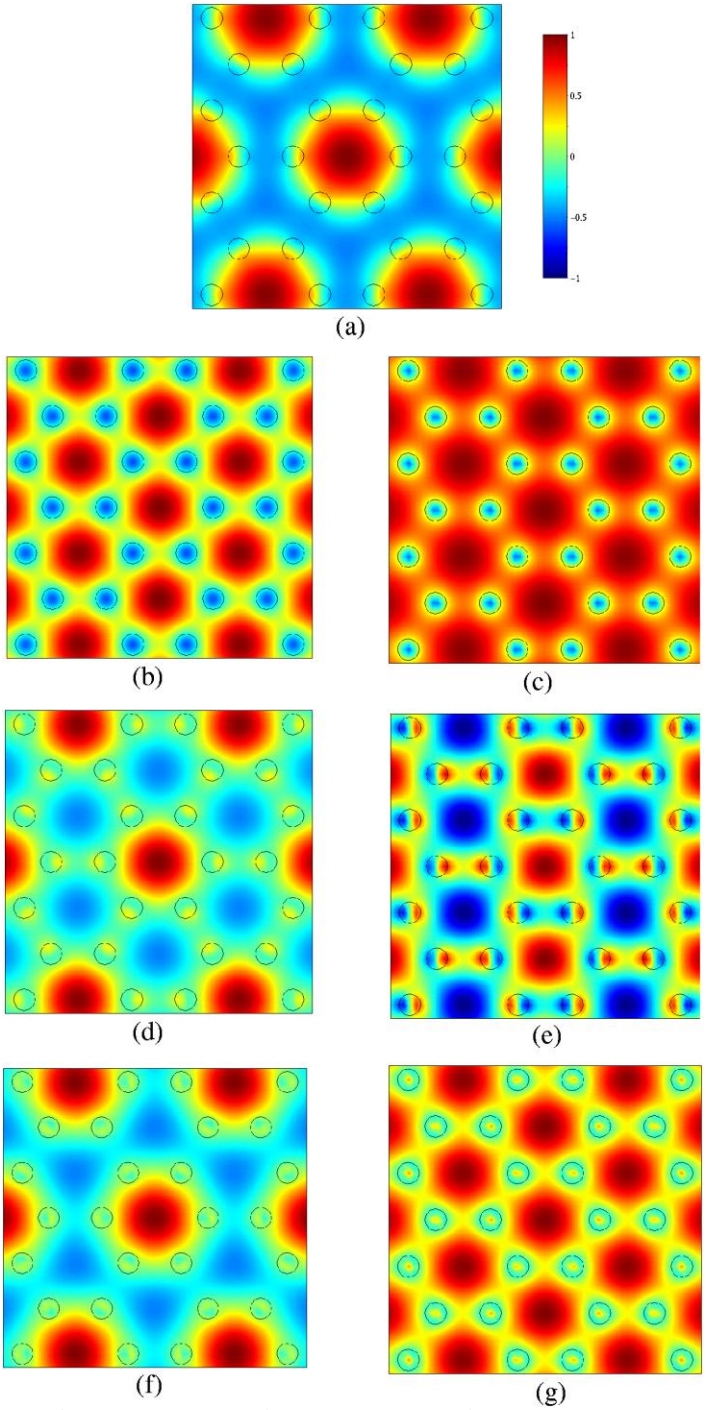

Fig. 8. One of the transverse electric field components (E_x) of Bloch states corresponding to the photonic bands' edge indicated by arrows from A to G in Fig. 7(b) is depicted from (a) to (g), respectively. The states of A, B, C, D, E, F, and G in Fig. 7(b) correspond to K, Γ, Γ, K, M, K, and Γ, respectively, and are composed of even state of LP_{11} rod modes, even state of LP_{02} rod modes, even state of LP_{02} rod modes, even state of LP_{12} rod modes, odd state of LP_{11} rod modes, even state of LP_{12} rod modes, and even state of LP_{03} rod modes, respectively.

#136546 - $15.00 USD Received 13 Oct 2010; revised 30 Dec 2010; accepted 11 Jan 2011; published 14 Jan 2011
(C) 2011 OSA

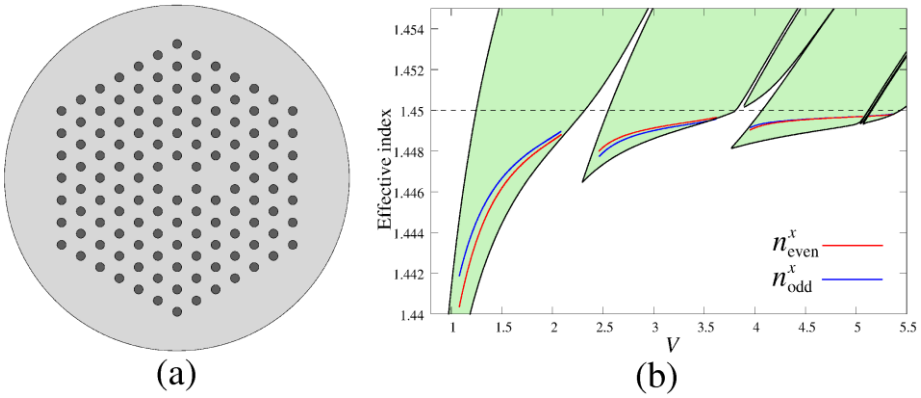

Fig. 9. (a) Cross section of conventional all-solid PBGF coupler with 2 cores. (b) Dispersion curves of the *x*-polarized even (red curves) and odd modes (blue curves) for the coupler, where the region with green represents the PBG of the triangular lattice for the first, second, and third-order PBGs (from left to right). Apparently, the effective index for the odd mode is larger in the odd-ordered PBGs.

3.2. Fundamental of novel concept "heterostructured cladding"

Because the proposed structure shown in Fig. 4(a) has a nonperiodic cladding contrary to the conventional all-solid PBGFs, attention should be given to the effect, as well as the consideration for the bands which the honeycomb lattice produces. In particular, the simultaneous realization of the single-mode operation and the low bending loss property for the proposed structure is due to the novel cladding concept "heterostructured cladding" [30]. In this section, we review the mechanism and the roles of the novel cladding concept in detail.

The proposed cladding structure shown in Fig. 4(a) can separately be considered as the two periodic cladding sections; that is, the triangular lattice from the 1st to 2nd ring (1st cladding) and the honeycomb cladding region from the 3rd to 6th ring (2nd cladding). Figure 10(a) shows the cross section of the structure which composes the 1st cladding of the proposed structure. In general, the property of a propagation angle range for which light is reflected at a boundary between a core and a cladding in an ideal PBGF with an infinite cladding is analogous to that in index-guiding conventional optical fibers [38,39], where the propagation angle is defined between the fiber axis and ray. If a periodicity of a photonic-crystal cladding in a PBGF is assumed, light is totally reflected at the boundary for propagation angles from 0 degrees to a critical angle which corresponds to a PBG edge. Although the cladding is finite in practical fibers, due to a lot of cladding layers in most situations, the property is very close to such a case, except for presence of the slight confinement loss. On the other hand, if the periodicity cannot be considered (such as the case that the cladding has only 2 rings), the property for the reflection at the boundary is very different from the previous case. Instead, the property becomes close to an anti-resonant reflection [23] or Fresnel reflection due to the destruction of the PBG concept. That is, as is well known in optics, the reflectivity attains almost 100% for light with the propagation angle of 0 degrees and it decreases gradually with the slight increment of the propagation angle (see Fig. 3 of Ref [24]. for example). Therefore, the mode confinement in the core by the 1st cladding is stronger for a mode with a larger effective index than for one with a smaller effective index, because the Fresnel reflection for light with a large propagation angle is poor. That is why the HOMs are effectively not confined in the 1st cladding. However, the fiber composed of only the 1st cladding cannot produce a tight confinement effect for the fundamental-like mode. In Fig. 10(b), we illustrate the cross section of the structure which is composed of only the 2nd cladding of the heterostructured cladding, while presenting the dispersion curves of the guided modes in the first-order PBG for the 2nd cladding structure in Fig. 11(a). The green region stands for the PBG of the honeycomb lattice. It is found that the

#136546 - $15.00 USD Received 13 Oct 2010; revised 30 Dec 2010; accepted 11 Jan 2011; published 14 Jan 2011
(C) 2011 OSA

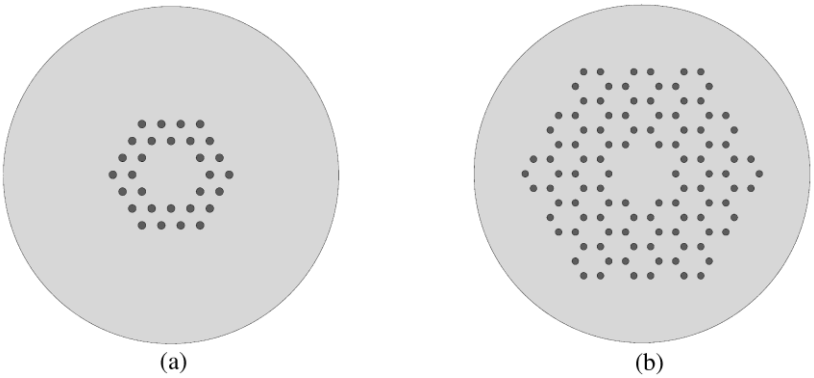

Fig. 10. Cross sections of the (a) uniform 7-cell-core structure with 2 rings which composes the 1st cladding and (b) structure with uniform honeycomb lattice cladding which composes the 2nd cladding of the heterostructure shown in Fig. 4(a).

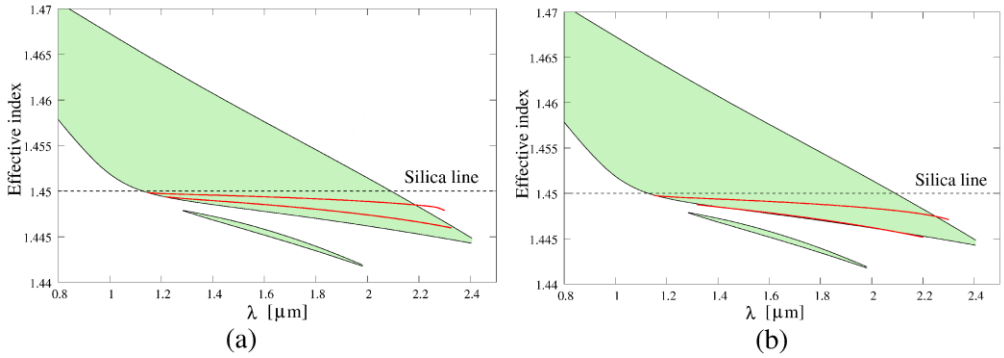

Fig. 11. (a) Dispersion curves of the fundamental-like and the HOM (HE_{21} mode) for the (a) 2nd cladding fiber shown in Fig. 10(b), and (b) proposed fiber with the heterostructured cladding shown in Fig. 4(a) in the first-order PBG (red curves), where the green region stands for the PBG of honeycomb lattice.

HOM exists in the PBG condition because of its large core size for the 2nd cladding fiber. Actually, we confirmed that the confinement loss of HE_{21} mode for such a fiber becomes less than 0.1 dB/m at the mid-gap wavelength. In Fig. 11(b), we present the dispersion curves of the guided modes in the first-order PBG for the proposed heterostructure shown in Fig. 4(a). Owing to the presence of the first cladding, the effective index for the guided modes is apparently reduced and, hence, the HOM is driven to the photonic band associated with the ARROW modes which the 2nd cladding produces. Thus, the 2nd cladding contributes to the tight confinement only for the fundamental-like mode in the heterostructured cladding.

It is noted that even if a fiber composed of only a 2nd cladding exhibits a high confinement loss property, as in [30], it is possible to reduce the bending loss by adding several rods around the core (forming the 1st cladding) with keeping the single-mode operation at the same time. This is the major first role of the heterostructured cladding structure. The second important role is to change the effective index for the 2nd cladding fiber into that at which the 2nd cladding structure is supposed to exhibit a single-mode operation by forming the 1st cladding with keeping a bending loss low, as shown above. In conclusion, only the fundamental-like mode is strongly confined in the core due to the fact that the HOMs experience a low reflectivity at the boundary between the core and the 1st cladding, and that the dispersion curves of the HOMs are driven to the resonant condition in the 2nd cladding, owing to presence of the 1st cladding. Therefore, simultaneous realization of the single-mode operation and the low bending loss property can be achieved by the heterostructured cladding with the 7-cell-core structure. It is also worth noting that the weak confinement for the HOMs

#136546 - $15.00 USD Received 13 Oct 2010; revised 30 Dec 2010; accepted 11 Jan 2011; published 14 Jan 2011
(C) 2011 OSA

in the 1st cladding attributed to the large propagation angle is essential for the single-mode operation, as mentioned above. Therefore, attention should be given to the value of effective indices when higher-order PBGs (like the third-order PBG) are exploited, where the effective index is larger (propagation angle is lower) in general.

4. Conclusions

In this work, we have proposed a novel mechanism for suppression of HOMs, namely multiple resonant coupling, in all-solid PBGFs with effectively large core diameters. We have shown that it contributes to a single mode operation at the first-order PBG without degradation of the bending property. In an analogy to the well-known tight-binding theory in solid-state physics, multiple ARROW modes bound in designedly arranged defects as a triangular lattice in the cladding make up Bloch states and resultant photonic bands with a finite effective-index width, which contribute to the suppression of HOMs. In particular, contrary to the conventional method for the HOM suppression using the index-matching, the proposed mechanism guarantees a broadband HOM suppression without a precise design of the defected cores set in the cladding. This effect is explained by the multiple resonant coupling, as well as the enhanced confinement loss mechanism which occurs near the condition satisfying the multiple resonant coupling. Moreover, we have shown that the proposed structure exhibits a lower bending loss characteristic when compared to the conventional all-solid PBGFs. The simultaneous realization of the single-mode operation and the low bending loss property is due to the novel cladding concept named as heterostructured cladding, which is constructed by two distinguishable structures. We demonstrated that the heterostructure contributes the following two main roles: Firstly, by forming the 1st cladding, the bending loss is reduced as compared to the structure constructed by only the 2nd cladding with keeping the single-mode operation at the same time. Secondly, by forming the 1st cladding, the effective index is changed for the 2nd cladding structure into that at which the 2nd cladding structure is supposed to exhibit a single-mode operation with keeping a bending loss low. That is, in the heterostructured cladding, HOMs are effectively suppressed in a large core due to the fact that the dispersion curves of the HOMs are driven to the resonant condition in the 2nd cladding, owing to presence of the 1st cladding. Moreover, it is achieved since HOMs with a large propagation angle are not tightly confined in the 1st cladding. In addition, we demonstrated the physical understanding of the formation of photonic bands induced by multiple ARROW modes in the honeycomb lattice for the first time, which contribute to the suppression of HOMs. The proposed structure also resolves the issue for the increased confinement loss property in the first-order PBG at the same time, without any particular complicated fabrication techniques except for the stack-and-draw ones.

The concept proposed here is based on the nonperiodic cladding contrary to the case for conventional PBGFs. This indicates that an improvement of the fiber properties by exploiting a non-uniform cladding is possible. In particular, although adopting the honeycomb lattice as the 2nd cladding has been considered for the heterostructure in this paper, various other combinations for the 1st and 2nd cladding could be applied to the proposed concept. In fact, we found that Kagome lattice also presents an analogous photonic bands induced by ARROW modes. Moreover, although the objective of this paper is to propose the fundamental concept for suppressing HOMs based on the novel mechanism named as multiple resonant coupling, it is important to show a structural optimization concerning the parameters of each high-index rod and the arrangement including the modified structure presented above. In terms of the parameters of each rod, we have shown the design principle for obtaining a low bending loss property for the 1-cell-core uniform structure on a fundamental level recently [40]. The optimization including the arrangement of the rods is an issue in the future.

Acknowledgements

The authors would like to kindly acknowledge the financial support of this project from the Japan Society for the Promotion of Science (JSPS), Grant-in-Aid for JSPS Fellows (20.2266).

#136546 - $15.00 USD Received 13 Oct 2010; revised 30 Dec 2010; accepted 11 Jan 2011; published 14 Jan 2011
(C) 2011 OSA